Dislocation-induced noise in semiconductors

2002 J. Phys.: Condens. Matter 14 13387

(http://iopscience.iop.org/0953-8984/14/48/393)

INSTITUTE OF PHYSICS PUBLISHING JOURNAL OF PHYSICS: CONDENSED MATTER

J. Phys.: Condens. Matter **14** (2002) 13387–13395 PII: S0953-8984(02)54242-9

Dislocation-induced noise in semiconductors

S Mil'shtein

Advanced Electronic Technology Center, ECE Dept. UMass, Lowell, MA 01854, USA

Received 3 October 2002
Published 22 November 2002
Online at stacks.iop.org/JPhysCM/14/13387

Abstract

Rapid advances in the semiconductor technology of nano-scale integration, optoelectronics for communication needs, and micromachines make the susceptibility of semiconductor systems to electronic noise a crucial issue. Electronic systems designed to carry high switching speed, large gain, and large power could be compromised by internally generated noise. Defects (especially extended) in crystalline structure are known to be sites of intense scattering and trapping in flows of carriers, and therefore are recognized as strong generators of noise in electronic materials and devices. Our study was focused on $1/f$ noise generated by dislocations. Even an extremely low level of this noise is rather disturbing to the operation of many electronic and optoelectronic devices.

In the current study a new noise figure of merit was introduced and applied in analysing the potential use of such materials as Si, Si–Ge, SiC, GaAs, GaN, and AlN. The potential low-noise performance of electronic materials is connected to the presence of extended crystalline defects, dislocations. A model was developed which links the magnitude of the recombination rate at the dislocation with fluctuation of the current, which could be measured by electron-beam-induced-current techniques. This model considers the dynamic change of the dislocation potential for a defect positioned inside an active area of a device, when the external bias changes at a p–n junction, at the gate of a field-effect-transistor or at the cavity of a laser.

1. Noise figure of merit

The selection of semiconductor materials for various applications is aided to a great extent by access to well-established figures of merit. A comparison of semiconductor properties is summarized in table 1. High-temperature electronics uses wide-gap semiconductors such as diamond ($E_g = 5.5$ eV) or AlN ($E_g = 6.2$ eV), and high frequency is possible in materials with high electron mobility such as GaAs ($\mu = 8500\ \mathrm{cm^2\ V^{-1}\ s^{-1}}$); high operational power can be utilized in materials with good thermal conductivity, such as diamond ($H = 22\ \mathrm{W\ cm^{-1}\ K^{-1}}$).

0953-8984/02/4813387+09$30.00

Table 1. Comparison of semiconductor properties (modified, after Morkoç *et al* 1994).

Property	Silicon	GaAs	β-SiC	4H-SiC	GaN	AlN	Diamond
Lattice constant (Å)	5.43	5.65	4.3596	$3.073a_0$ $10.053c_0$	4.51	$3.11a_0$ $4.979c_0$	3.567
Thermal expansion (10^{-6} °C)	2.6	5.9	4.7	$4.2a_0$ $4.68c_0$	5.6	$4.5a_0$	0.08
Density (g cm^{-3})	2.328		3.210	3.211	6.095	3.255	3.515
Melting point (°C)	1420		2830	2830			4000
Band gap (eV)	1.1	1.43	2.2	3.26	3.45	6.2	5.45
Saturated electron velocity (10^7 cm s^{-1})	1.0	1.0	2.2	2.0	2.2	?	2.7
Electron mobility (cm^2 V^{-1} s^{-1})	1500	8500	1000	1140	1250	?	2200
Hole mobility (cm^2 V^{-1} s^{-1})	600	400	50	50	850	?	1600
Breakdown (10^5 V cm^{-1})	3	6	20	30	>10	?	100
Dielectric constant	11.8	12.5	9.7	9.6/10	9	8.5	5.5
Resistivity (Ω cm)	1000	10^2	150	$>10^{12}$	$>10^{10}$	$>10^{13}$	$>10^{13}$
Thermal conductivity (W cm^{-1} K^{-1})	1.5	0.46	4.9	4.9	1.3	3.0	22
Absorption edge (μm)	1.4	0.85	0.50	0.37	0.36	0.12	0.22
Refractive index	3.5	3.4	2.7	2.7		3.32	2.42
Hardness (kg mm^{-2})	1000	600	3980	$2130c_0$		1200	10 000
Johnson's figure of merit (10^{23} WΩ s^2)	9.0	62.5	2533	4410	15 670	?	73 856
Keyes' figure of merit ($\times 10^2$ W cm^{-1} s^{-1} °C)	13.8	6.3	90.3	229	118	?	444
Baliga's figure of merit (relative to silicon)	1.0	15.7	4.4		24.6	?	101
Temperature figure of merit	220	394	650	815	1060	3000	2727
Noise figure of merit (10^3)	6.7	1.2	22	17.5	17.6	26.6	12.3

We introduce a new noise figure of merit (NFOM), which allows us to assess the future application of a technology using a given material. The conventional relation between the electron mobility μ and the saturation velocity $v = \mu\varepsilon$ is controlled by the electrical field.

For a given electrical field, larger mobility μ should produce larger v for a given material. Deviation from this simple rule is typically caused by special features of the E–k diagram and/or phonon spectra, i.e. by intense scattering/recombination processes. Comparison of Si with GaAs provides an example of deviation from the rule. Comparison of β-SiC and GaN is a similar example. We suggest using the ratio of saturation velocity to carrier mobility as the noise figure of merit:

$$\text{NFOM} = (v/\mu) \times 10^3. \tag{1}$$

The last, separate line in table 1 gives the NFOM for a few semiconductor materials. The inherited properties of a material, such as the presence of various defects, clearly modify the phonon energy distribution and this should be reflected in the intensity of the scattering and/or trapping, which in turn could cause a higher level of noise. In our opinion, a lower value of the NFOM suggests limiting a given material to use in design and fabrication of low-noise electronic devices. According to the NFOM, β-SiC is better than GaN; however, AlN is expected to outperform other materials in the manufacturing of low-noise electronic devices.

Our study was focused on one of the most important cases of noise distortion, namely, on $1/f$ noise and on the role of linear defects in the generation of this type of noise. This

noise is observed in both electronic and optoelectronic devices. Although the mechanisms of electron-trap interaction in optical detectors are clearly different to those in FETs, a unique $1/f$ dependence is observed in all experimental studies of both device groups (Van Der Ziel 1975). Very often this noise is called phase or flicker noise.

Flicker noise (or $1/f$ noise) is a very important type of noise in electronic systems used in radar in airports, in cars, and in all systems where the Doppler signal becomes smaller in amplitude than the $1/f$ noise. With the increased volume of air traffic and larger numbers of cars on the roads, the level of electronic noise is increasing to the point where noise filtering circuits are at the limits of performance, and noise immunity of the system should be provided by reduction of the internal noise of amplifiers, i.e., the internal noise of transistors. The typically acceptable internal noise in these systems is far below zero, about -120 dB. Currently many R&D groups are involved in the development of electronic systems with even lower levels of this noise. We analysed the model of the trapping dislocation potential and its behaviour in semiconductor devices when an external bias was applied, as well as the possibility of measuring the noise level directly using the electron-beam-induced-current (EBIC) technique.

2. Recombination–generation process

Excess carriers generated by light, heat, or an electron beam in the scanning electron microscope (SEM) quickly recombine at defects in crystals. In the current study, we considered dislocation-induced $1/f$ noise and the correlation between the level of noise and the magnitude of the recombination rate. The EBIC technique, widely used (Leamy 1982) for the imaging of extended defects, produces dark contrast along a defect, where the intensity of the contrast is proportional to the rate of recombination of electron–hole pairs. EBIC contrast is expressed in percentage units, i.e. the value of the contrast is by definition a relative parameter.

When the beam in the SEM scans the device under test, electron–hole pairs are generated in a volume defined by the electron range. We consider n-type material with holes being the minority carriers. As the recombination of carriers takes place at the defect site, a proportional current flux, collected by a Schottky diode, forms the EBIC signal (Mil'shtein *et al* 1984). All such events can be modelled using the Boltzmann continuity equation (BCE), which describes the behaviour of the excess carriers (δp) (Neamen 1997):

$$D_p \frac{\partial^2(\delta p)}{\partial x^2} - \mu_p \bar{E} \frac{\partial(\delta p)}{\partial x} + g - \frac{\delta p}{\tau_{p0}} = \frac{\partial(\delta p)}{\partial t} \tag{2}$$

where δp is the density of excess minority carriers, μ_p is the mobility of carriers, D_p is the diffusivity of carriers, τ_{p0} is the lifetime of carriers, and $\bar{E}$ is the electrical field within a Schottky barrier.

In order to apply equation (2) in quantitative measurement of the recombination rate at a given defect site, one should, first, identify the terms of the equation relating to the EBIC process and, secondly, simplify this expression as far as possible. The generation function g, which defines how many electron–hole pairs are produced by the beam, can be defined as

$$g = I_b M \tag{3}$$

where I_b is the primary electron beam current and M is a multiplication factor, which can be accessed via knowledge of the acceleration energy (in eV) of the microscope and the energy gap (in eV) of the semiconductor material under test. The assessment of the generation function and use of the BCE imposes certain disadvantages in comparison with Monte Carlo analysis. The BCE method does not address the spatial distribution of secondary electrons in the electron range volume. That could be a serious limitation when the modelling describes high-resolution

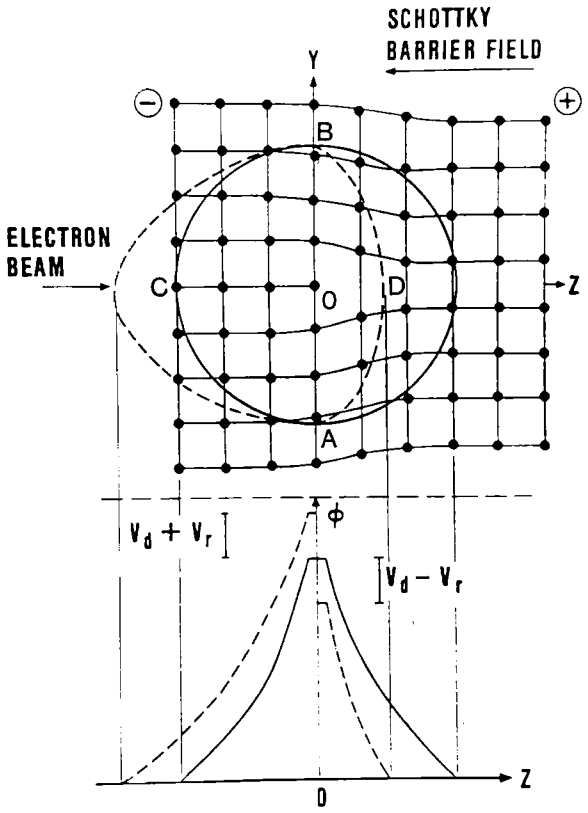

Figure 1. Changes of the space charge (a) and the electrostatic potential (b) around a 90° dislocation with changing electrical field (modified, after Matare1971); ——: without external bias; - - - -: with bias applied.

EBIC measurements. The recombination term $\delta p/\tau_0$ depends on the spatial distribution of the carriers generated as well. The first and second terms in equation (2) represent the diffusion and drift current inside the collecting (Schottky) device. Under equilibrium conditions, the diffusion and drift currents are equal to $g - \delta p/\tau_{p0}$ and constitute the EBIC signal:

$$I_{EBIC} = D_p \frac{\partial^2(\delta p)}{\partial x^2} - M_p \bar{E} \frac{\partial(\delta p)}{\partial x}. \tag{4}$$

For steady conditions—for example, when the electron beam does not move—$\partial(\delta p)/\partial t = 0$.

3. Dislocations as generators of noise

A dislocation line (see figure 1(a)) along the x-direction presents a set of dangling bonds. The electrons trapped along the dislocation line present a linear negative potential surrounded by a cylinder depleted of free electrons. The base of the cylinder and its side surface represent the defect cross-section, measured in cm^2. The radius of such a cylinder can be assessed by calculation of the Debye screening length (Mil'shtein 1979) and in doped material still represents a fraction of a micrometre. The electrostatic potential might reach 1 eV, as measured

by our group (Mil'shtein 1985). The solid curves in figure 1 depict the shape of the electric field (see figure 1(a)) and the height of the electrostatic potential (see figure 1(b)) with no external bias. The dashed curves in figure 1 are contours of the potential with an external bias applied.

Applying the field along the diameter of the circle will increase the electrostatic potential of the dislocation on one side and decrease the potential on the other side, turning the circular base into an elliptical base (see the dashed contour in figure 1). So application of an external field increases the cross-section of the defect and, as a result, the recombination–generation rate increases. In other words, biasing of electronic device 'provokes' trapping activities of a defect.

4. Correlation between the $1/f$ noise and recombination rate

The recombination rate in the Boltzmann equation (2) is governed by the velocity of the tunnelling electrons v, the cross-section of traps S, and the trap density N_{traps}:

$$\frac{\delta p}{\tau} = \frac{\delta p}{v S_{traps} N_{traps}}. \tag{5}$$

Following recent $1/f$ modelling (Luo *et al* 1988), the spectral density of $1/f$ noise being normalized to a current through a gate junction (the EBIC current) can be expressed as follows:

$$\frac{S(f)}{I_{EBIC}^2} = \left(\frac{v_t}{v_d}\right)^2 \frac{q^2 W}{3\varepsilon K T A} \exp\left(\frac{q^2 N_D W^2}{2\varepsilon K T}\right) \frac{\alpha_H}{f} \tag{6}$$

where $v_t = (KT/2\pi m^*)^{1/2}$ is the generation–recombination velocity, v_d is the diffusion velocity, W is the width of the depleted region, α_H is the Hooge parameter, T is the lattice temperature, A is the gate area, N_D is the doping concentration, I_{EBIC} is the current through the gate, f is the frequency.

The diffusion velocity v_d defined by equation (5) links the magnitude of the rate of recombination at defects to the amplitude and spectra of the $1/f$ noise. One should note that the width of the depleted region is a function of the gate and drain voltages, $W = f(V_g^{1/2}, V_D^{1/2})$, and it is present before the exponent as well as in the exponential term; therefore an increase of the biases at gate and drain terminals (i.e. an increase of the field in a transistor) will significantly increase the noise amplitude.

5. Quantitative measurements of the recombination rate using EBIC

The measured EBIC contrast is defined as

$$\frac{I_{EBIC} - I_{0EBIC}}{I_{0EBIC}} = C\ (\%) \tag{7}$$

where I_{0EBIC} is the signal from the background surrounding the defect under test, I_{EBIC} is the signal from the defect.

The relative nature of the contrast measurements could be presented in a different manner. After all, the contrast is a multi-parameter function: $C(E, I_b, R_e, \Sigma, I_{leak}, V_r, W, L, X_d, \varphi_d)$, where E is the accelerating voltage, I_b is the beam current, and R_e is the electron range (these are parameters of the beam); Σ and I_{leak} are the collection efficiency and the leakage current respectively of a Schottky barrier, and V_r is the bias (these are parameters of a gate junction); W is the width of the depleted region, and L is the minority carrier diffusion length (these are parameters of a semiconductor material); X_d is the position of a defect relative to the surface

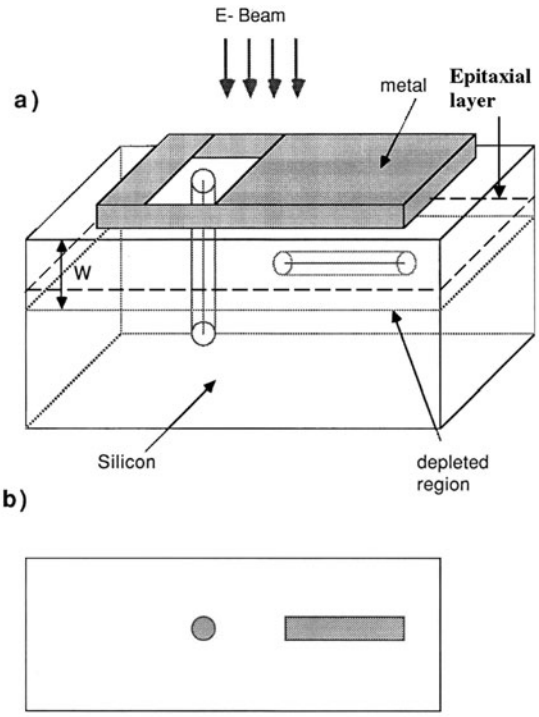

Figure 2. Two dislocations under the gate. (a) Threading and misfit dislocations. (b) A SEM projection of the dislocations.

of a specimen, and φ_d is the electrical potential of a defect (these are parameters of the defect). The complexity of the contrast function together with equation (6) emphasizes the relative nature of the EBIC signal. The first step in the direction of quantitative measurements is to minimize the number of parameters which are changing in the experiments, and to scan only the defect, avoiding scanning of the background.

Combining equations (2)–(4), one can write

$$I_{EBIC} + I_b M - \frac{\delta p}{\tau} = 0 \tag{8}$$

where the recombination rate

$$\frac{\delta p}{\tau} = I_{EBIC} + I_B M. \tag{9}$$

Now, scanning along the same dislocation line twice for two different intensities of the primary electron beam, we obtain the change of the recombination rate:

$$\Delta \frac{\delta p}{\partial \tau} = I_{EBIC1} + I_{b1} M - I_{EBIC2} + I_{b2} M. \tag{10}$$

Keeping the same bias of the collecting junction keeps Σ, I_{leak}, V_r, W, L, X_d, φ_d unchanged. Keeping the same acceleration voltage keeps R_e unchanged. Changing I_{b1} and I_{b2} allows one to measure the change of the recombination rate quantitatively. To simplify the measurement of $\Delta \frac{\delta p}{\tau}$ further, one should take an image of the defect with beam intensity I_{b1} and subtract a second image taken with beam intensity I_{b2}.

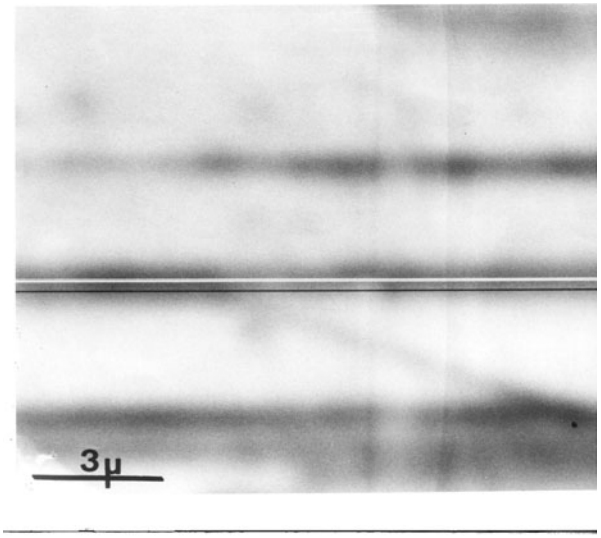

Figure 3. An EBIC scan of a single dislocation parallel to the surface of a sample.

Figure 2 depicts the metal gate and the channel with a depleted region of depth W produced by the epitaxial process. Substrate mismatch with the epitaxial layer generates the threading and misfit dislocations shown in figure 2(a). Figure 2(b) presents dark-contrast images for both dislocations. Figure 3 shows an example of an EBIC line scan.

Performing quantitative EBIC measurements along the misfit dislocation line or across a dot image of a threading dislocation, knowing the density of dislocations in the area examined, will allow assessment of the intensity of recombination per unit of volume and, based on that, calculation of the level of noise.

6. Summary

The appearance of a dark field (EBIC contrast) around a dislocation (see the magnified line scan in figure 3) is a manifestation of a noise contribution of a given dislocation to the collective (integral) noise generated by all linear defects.

To simplify the discussion and equation (6), the spectral density of $1/f$ noise can be presented in the form

$$\bar{i}^2 = S(f) * \Delta f = K_f * \Delta f * I^\alpha / I \tag{11}$$

where Δf is a small bandwidth at frequency f; I is the current through the gate (EBIC current); K_f is a constant for a particular device, which depends on the density of crystal defects; α is a constant in a range 0.5–2; for $\beta = 1$ the noise spectral density is approximately proportional to $1/f$.

In field-effect transistors, such as MESFETs, the interface traps under the gate are the most important contributors to the noise. They generate the fluctuation of the current I_s in the reverse-biased Schottky gate diode. Measuring the average saturation reverse current I_s, one can assess the spectral noise density through the value of i^2:

$$\bar{i}^2 = \overline{(I - I_s)}^2 = \lim \frac{1}{T} \int_0^T (I - I_s)^2 \, \mathrm{d}t. \tag{12}$$

The question of whether the EBIC is reflected in the level of noise induced by linear defects remains open. Identification of current values in equations (6), (11), and (12) is essential for understanding the EBIC process. Measurements of a background EBIC I_{0EBIC} can identify all defect contributions to the average leakage current $I_S = I_{0EBIC}$. An EBIC scan along a given dislocation will allow measurement of $I_{EBIC} = I$. In other words, the value i^2 can be directly derived from EBIC measurements. The limit of integration T is controlled by the beam scanning rate. Overall direct measurements of the recombination rates at defect sites would provide an assessment of the noise intensity. In attempts to measure the spectral density $S(f)$ of the I/f noise by the EBIC technique, one should use a beam blinking system to emulate the signals of a certain frequency which arrive at the gate of a MESFET under operational conditions. Thus by changing the frequency of the EBIC signal, one can obtain $1/f$ noise spectra where absolute (not relative) values of $S(f)$ are linked to the intensity of recombination of electron–hole pairs at the defect site.

Variation of contrast along a single dislocation is further proof of current fluctuation (noise) induced by defects. One of the fundamental unresolved issues in the theory of $1/f$ noise is the undefined role of the current through the transistor or the voltage applied to the terminals of the device, i.e., the dominant role of the current or electrical field in the formation of noise. The operation of any FET is governed by the current being a nonlinear function of the gate and drain biases applied, i.e., current being a function of the electrical field established in the channel of a transistor. The dislocation trapping potential is also exposed to and changes with changes of the field along the channel of a FET. Therefore, we conclude that the dominant role of the electrical field in the noise generation process is obvious, although the spectral noise density is commonly expressed through the current value i^2:

$$\bar{i}^2 = \left(\frac{\overline{I_{EBIC} - I_{0EBIC}}}{I^2_{0EBIC}} \right)^2. \tag{13}$$

The average EBIC contrast $\bar{C}^2$ is effectively the normalized root mean square value of the EBIC expressed in equation (13).

7. Conclusions

We modelled in this study the link between $1/f$ noise spectra and the diffusion velocity. In turn, v_d is connected to the recombination rate (equation (5)). We proposed a novel experimental procedure for making quantitative measurements of the recombination rate using the EBIC technique. We plan to try making these measurements on a transistor structure in the near future; the EBIC results will be correlated with measurements of the $1/f$ noise.

Acknowledgment

This work was supported by a grant from Raytheon Co.

References

Ghandhi S 1994 *VLSI Fabrication Principles* (New York: Wiley) p 258

Kumar A, Kalra E, Maldar S and Gupta R 2000 $1/f$ noise model of fully overlapped lightly doped drain MOSFET *IEEE Trans. Electron Devices* **47** 1426

Leamy H 1982 Charge collection scanning electron microscopy *J. Appl. Phys.* **53** R51

Luo M, Bosman G, Van Der Ziel A and Hench L 1988 Theory and experiments of $1/f$ noise in Schottky-barrier diodes operating in the thermionic-emission mode *IEEE Trans. Electron Devices* **35** 1351

Matare H 1971 *Defect Electronics in Semiconductors* (New York: Wiley) p 431
Mil'shtein S 1979 Applications of dislocation-induced electric potentials *J. Physique* **40** 207–211
Mil'shtein S 1985 Dislocation trapping potential measured by SEM-CCM *Mater. Res. Soc. Symp. Proc.* **46** 487–92
Mil'shtein S 2001 Quantitative EBIC measurements *Patent Application*
Mil'shtein S, Joy D, Ferris S and Kimerling L 1984 Defect characterization using SEM-CCM *Phys. Status Solidi* a **84** 363–9
Morkoç H, Strite S, Gao G, Lin M, Sverdlov B and Burns M 1994 Large-band-gap SiC, III–V nitrides and ZnS-based semiconductor device technologies *J. Appl. Phys.* **76** 1363
Neamen D 1997 *Semiconductor Physics and Devices* (Boston, MA: Irwin) p 173
Van Der Ziel A 1975 *Noise in Measurements* (New York: Wiley) p 21